

Cellular prion protein PRPC and ecto-5'-nucleotidase are markers of the cellular stress response to aneuploidy

Patrícia H. Domingues¹, Lalitha S. Y. Nanduri^{1,2}, Katarzyna Seget^{3,4}, Sharavan V. Venkateswaran⁵, David Agorku¹, Cristina Viganó⁶, Conrad von Schubert⁶, Erich A. Nigg⁶, Charles Swanton⁷, Rocío Sotillo⁵, Andreas Bosio¹, Zuzana Storchová^{3,4} and Olaf Hardt^{1,*}

1 Miltenyi Biotec GmbH, Bergisch Gladbach, Germany

2 Amrita Centre for Nanosciences and Molecular Medicine, Amrita Vishwa Vidyapeetham, Kochi, Kerala, India

3 Group Maintenance of Genome Stability, Max Planck Institute of Biochemistry, Martinsried, Germany

4 Department of Molecular Genetics, University of Kaiserslautern, Kaiserslautern, Germany

5 Division of Molecular Thoracic Oncology, Deutsches Krebsforschungszentrum (DKFZ), Heidelberg, Germany

6 Biozentrum, University of Basel, Basel, Switzerland

7 Translational Cancer Therapeutics Laboratory, Francis Crick Institute, London, United Kingdom

*Corresponding author

Postal address:

Olaf Hardt

Miltenyi Biotec GmbH

Friedrich-Ebert-Str. 68

51429 Bergisch Gladbach

Germany

Phone +49 2204 8306-4212

Fax +49 2204 8306-5727

olaf.hardt@miltenyibiotec.de

Running Title: Cell surface proteome of aneuploid cells

Key words: Aneuploidy, biomarker, cellular stress, cellular prion protein, PRPC, CD73, ecto-5'-nucleotidase

Financial support

This work was supported by the Marie Curie Network PloidyNet, funded by the European Union Seventh Framework Programme (FP7/2007-2013) under Grant Agreement n°316964 (to Patrícia H. Domingues, Lalitha S. Y. Nanduri, Katarzyna Seget, Sharavan V. Venkateswaran, Cristina Viganó, Conrad von Schubert, Erich A. Nigg, Charles Swanton, Rocío Sotillo, Zuzana Storchová and Olaf Hardt). The funders had no role in study design, data collection and analysis, decision to publish, or preparation of the manuscript.

Abstract

Aneuploidy is a hallmark of most human tumors, but the molecular physiology of aneuploid cells is not well characterized. In this study, we screened cell surface biomarkers of ~300 proteins by multiparameter flow cytometry using multiple aneuploid model systems such as cell lines, patient samples and mouse models. Several new biomarkers were identified with altered expression in aneuploid cells, including overexpression of the cellular prion protein CD230/PRPC and the immunosuppressive cell surface enzyme ecto-5'-nucleotidase CD73. Functional analyses associated these alterations with increased cellular stress. An increased number of CD73+ cells was observed in confluent cultures in aneuploid cells relative to their diploid counterparts. An elevated expression in CD230/PRPC was observed in serum-deprived cells in association with increased generation of reactive oxygen species. Overall, our work identified biomarkers of aneuploid karyotypes which suggest insights into the underlying molecular physiology of aneuploid cells.

Introduction

Aneuploidy refers to an abnormal chromosome number that differs from multiples of the haploid set. Due to its negative effect on cellular physiology, it is considered to be the leading cause of spontaneous miscarriages in humans and can cause pathological conditions such as trisomy syndromes (e.g. Down's syndrome, trisomy of chromosome 21) and mosaic variegated aneuploidy (1). In addition, aneuploidy has also been tightly associated with cancer and, in contrast to cases with trisomy syndromes, malignant tumors often show variable aneuploid karyotypes with no apparent adverse effect on cell proliferation (2). In fact, it has been hypothesized that aneuploidy *in vivo* facilitates tumorigenesis and generates phenotypic variation, thus providing a growth advantage under selective conditions (3,4). Such phenotypic heterogeneity arises mainly from chromosomal instability (CIN), which is characterized by increased rate of loss/gain of whole chromosomes or parts thereof. In tumor cells, aneuploidy is often accompanied by CIN, which provides a mechanism to boost tumor progression due to emergence of cells with growth or survival advantages, the driving force of cancer development (5). This might be the reason why, in many types of cancer, higher levels of aneuploidy have been associated with poor prognostic factors such as higher tumor grade, tumor recurrence, metastasis and decreased overall patient survival (6).

The identification of biomarkers related to aneuploidy, or even to specific characteristics of aneuploid cells that may allow them to survive under specific conditions such as cellular stress, would not only increase our insight into its biological background, but would also facilitate the development of an early screening tool to detect and/or quantify aneuploidy in tumors, ultimately improving the clinical management of cancer patients. In line with this, a major focus of current research is to determine how cells respond to gene expression imbalances that are caused by aneuploidy (7,8). In the past years, global genome, transcriptome and proteome studies in aneuploid models as well as in cancers have provided new insights into the cellular response to aneuploidy (7-13). Such studies indicate that copy number variations (CNV) of specific chromosomal regions can alter the expression of genes located on those regions. At the same time, aneuploidy *per se* can affect the transcription of many genes across the entire genome due to activation/inhibition of multiple pathways (11,12). Similarly, protein levels also scale with the gene copy number (CN), although it should be noted that some of the proteins coded on extra chromosomes

are compensated by post-translational mechanisms that attenuate their levels when their encoding genes are in excess (e.g. subunits of macromolecular protein complexes and kinases) (7,8). However, the exact cellular and physiological responses to aneuploidy are incompletely understood. In the past years, several new models have been established in order to decipher the consequences of aneuploidy. These include mouse models (14), human tri/tetrasomic cells generated by introducing one or more individual chromosomes into a host cell, and embryo- and patient-derived cell lines with trisomy syndromes (2).

In this study, we aimed at identifying cell surface biomarkers correlated with an aneuploid karyotype by analyzing multiple models of aneuploidy for expression of approximately 300 proteins by multi-parameter flow cytometry (MFC). This approach allows for the measurement of multiple features on a single cell level and thereby a direct analysis of cell surface marker expression, which makes it a powerful method not only for the immunophenotypic characterization of cells, but also for the identification of novel biomarkers. In the study presented here, several new biomarkers have been identified to be associated with an aneuploid karyotype. Functional analysis showed that the main candidates were associated with the response to specific stress conditions, such as oxidative stress. Taken together, our findings provide novel tools to detect and analyze cells with aneuploid chromosome settings, as well as additional functional insight into the subsequent cellular stress arising in response to aneuploidy.

Material and Methods

Cell lines, patients' fibroblasts and culture conditions

The aneuploid cell lines used as a model in the present study were generated from the parental cell line HCT116 (human colorectal carcinoma cell line) - HCT116 13/3 (trisomy 13; clones 2-3), HCT116 18/3 (trisomy 18; clones 1-2) and HCT116 21/3 (trisomy 21; clones 1 and 3) -, the parental cell line HCT116 H2B-GFP - HCT116 3/3 (trisomy 3; clones 11 and 13), HCT116 5/3 (trisomy 5), HCT116 8/3 (trisomy 8; clones 3, 5 and 7), HCT116 5/4 (tetrasomy 5) and HPT (post-tetraploid; clones 1, 2 and 4) -, the parental cell line RPE1 (human retinal pigment epithelial cell line, hTERT immortalized) - RPE1 3/3 (trisomy 3; clone 1), RPE1 5/3 (trisomy 5; clone 3 and 7), RPE1 12/3 (trisomy 12) and RPE1 5/3 12/3 (trisomy 5, 12) -, the parental cell line RPE1 H2B-GFP - RPE1 3/3 (trisomy 3; clone 2), RPE1 21/3 (trisomy 21) and RPT (post-tetraploid; clones 1, 3 and 4) -, and the parental cell line DLD1 (human colon adenocarcinoma cell line) - post-tetraploids with karyotype near-3N (clones 7, 13, 16), 4N and >4N -. All tri- and tetrasomic cell lines were generated by microcell mediated chromosome transfer (MCMT) as described previously and verified by sequencing (7,11,15,16). The post-tetraploid HPT and RPT cell lines were generated by expansion of individual tetraploid clones after inhibition of cytokinesis through dihydrocytochalasin D (DCD, Sigma-Aldrich, St. Louis, MO, USA) treatment, and the DNA content was confirmed by flow cytometry, standard karyotyping, chromosome painting and array comparative genomic hybridization as previously described (11,17). Additional tetraploid clones were generated previously by FACS-sorting of spontaneously arising tetraploids within the HCT116 population (18). Diploid and tetraploid DLD1 cell lines were described previously (19) and spontaneously arising post-tetraploids were selected from the tetraploid population by FACS sorting, as described in detail elsewhere (20 and Viganó *et al.*, unpublished). All the cell lines were tested for mycoplasma contamination. Table 1 includes an overview of all cell lines included in the study, with the corresponding karyotype and clones, as well as reference of origin. Cells were cultured in Dulbecco's Modified Eagle Medium (DMEM high glucose, Gibco), supplemented with 10% fetal calf serum (FCS), 100U penicillin and 100U streptomycin (LONZA) and maintained at 37°C with 5% CO₂ atmosphere. Fibroblasts from patients with trisomy syndromes were purchased from the Coriell Institute (Camden, New Jersey, USA), with +21 karyotype (No. GM01137A, GM02767D and AG06872A), +18

karyotype (No. AG12614 and GM03538) and +13 karyotype (No. AG10292), and maintained in culture according to suppliers' specifications (<http://catalog.coriell.org>). IMR-90 (#CCL-186, ATCC, Manassas, VA) normal human fibroblasts were used as control. Cells were detached using either Trypsin-EDTA (Sigma-Aldrich), or Accutase (Merck Millipore, Billerica, MA, USA) for the cell surface marker screenings, followed by centrifugation at 300 g for 5 min.

Mouse models of aneuploidy

Mouse tumors were obtained from *TetO-Her2*, *TetO-KrasG12D/MMTV-rtTA* with and without *Mad2* overexpression (21) as well as a new transgenic animal model *TetO-PLK1/TetO-Her2/MMTV-rtTA* (Venkateswaran *et al.* unpublished). Single cells obtained from these tumors were injected into the cleared mammary fat pad of *Rag2*^{-/-} mice (22) maintained on a doxycycline diet to regrow the primary tumor. Surgical procedures were performed under isoflurane inhalation (2.5% in 0.8 L/min, Esteve) and in accordance with local disinfection and sterilization guidelines. R1 and R15 tumors used in the study had a *Kras* genotype, R16 and R10 a *Kras/Mad2*, R4 and R5 a *PLK1/Her2*, and the R3 had a *Her2* genotype. The tumors were genetically characterized as previously described (21): R10 (whole-chromosome gain of chromosomes 1 and 8 and loss of chromosomes 4, 5, 9, 10, 14, 16, 18 and x), R5 (gains of chromosomes 6 and 18, loss of chromosome 16 and a complex rearrangement on 10) and R4 (gains of chromosomes 1, 3 and 18) tumors were highly aneuploid, while R16 (loss of chromosome 4), R1 and R15 (no SCNA identified by WGS) were considered low aneuploid tumors.

Cell surface marker screening of aneuploid cells

Cells were analyzed using the MACS[®] Marker Screen, human (Miltenyi Biotec, Bergisch Gladbach, Germany) containing 300 antibodies (Ab) APC-conjugated - 291 antibodies specific for surface proteins plus 9 isotype controls (Supplementary Table S1), arrayed in four U-bottom 96-well plates (one Ab/well). Before staining, lyophilized Abs were reconstituted with 25µL/well of deionized water. Cells were stained at a density of 0.5-2x10⁵ cells per well in 50µL volume of PBS pH 7.2, 2 mM EDTA and 0,5% BSA (PEB) buffer at 2-8°C for 10 min, followed by 2 washing steps with PEB. To analyze four cell lines simultaneously per screening, cells were labeled using CellTrace™ Violet and/or CFSE (Life Technologies, Carlsbad, CA, USA) at concentrations of 0.5-3 µM before the Ab staining, according to the manufacturer's

instructions, and later gated in a V1(VioBlue)-A vs B1(FITC)-A plot. For those cell lines expressing H2B-GFP, only CellTrace™ Violet was used. Analysis was performed using the MACSQuant™ Analyzer and data analysis using the MACSQuatify™ software (Miltenyi Biotec). Propidium iodide (PI, 1 μ g/mL) was used as viability dye. For validation screenings, a specific panel was established (Supplementary Table S2) and cells were stained as previous with an antibody dilution of 1:10.

It is known that some aneuploid cell lines are larger than their euploid counterparts. In the flow cytometer used in our study, cells are investigated inside of a well-defined three-dimensional region. This region is defined in one dimension by the hydrodynamically focused core stream carrying all cells with a diameter typically smaller than 15 μ m. Cells can be larger than 15 μ m in their natural environment or in an adherent state, however, when dissociated and put into a single cell suspension, cells round up and are significantly smaller. In the two other dimensions it is defined by the intersection of the laser excited volume and perpendicular to it by the volume imaged onto the light detector tubes (PMT). The resulting “observed volume” is in the order of 15 μ m x 15 μ m x 15 μ m and has a fuzzy boundary. All fluorescence inside of that volume are taken into account for quantitation. The remaining unbound molecules within that volume, are quantified as well as all fluorescent molecules bound to the cell. The background signal is then subtracted from the signal collected while a cell is present. Thus, if there is a significant background contribution (e.g. by unbound fluorochrome-conjugates), a larger cell will displace more of that than a smaller cell. But other than that, the total fluorescence is detected independent from the cell size, as long as the cell fits completely in said observed volume. As a consequence, the measured signal is proportional to the total number of molecules bound to the cell, independent from cell-size. To verify this theoretical prediction and to exclude a bias of the cell size on the fluorescence intensity of the cell surface marker staining, we have plotted FSC signals versus fluorescence signals and observed no correlation (data not shown). Concerning the issue of unbound dyes, unstained cells are the best control, since a larger unstained cell population will displace more unbound particles and as a consequence should have a lower (even negative) average mean fluorescence when compared to smaller cells. We included unstained controls for every cell line analyzed without observing this issue.

Cell surface marker screening of mouse tumors

Tumor tissue was dissociated into a single cell suspension using the Tumor Dissociation Kit, mouse (Miltenyi Biotec), in combination with the gentleMACS Octo Dissociator with heaters (Miltenyi Biotec) according to the manufacturer's instructions. CellTrace™ Violet (Life Technologies) staining was used as previously described in order to analyze simultaneously two tissue samples (tumor and/or normal mammary gland) per screening, followed by staining with a cocktail of monoclonal antibodies for non-tumor cell exclusion (CD45, clone 30F11; Ter119, clone Ter-119; CD31, clone 390; CD90.2, clone 30-H12; conjugated to APC or FITC; dilution 1:10, all Miltenyi Biotec). Cells were then stained with a panel of 29 cell surface mouse antibodies plus 7 isotype controls PE-conjugated, arrayed in a U-bottom 96-well plate (Supplementary Table S3).

siRNA-mediated knockdown

For knockdown of expression of candidate genes, HCT116 (parental cells, control) and HPT1-H2B GFP (selected as representative for aneuploidy) cells were transfected with small interfering RNAs (siRNAs) using MACSfectin™ Reagent (Miltenyi Biotec). A mixture of four small interfering RNAs (ON-TARGETplus SMARTpool siRNAs) for NT5E (CD73; 4905), PRNP (CD230; 5621), CD55 (1604), FAS (CD95; 355), CD47 (961) and ITGA2 (CD49b; 3673) were obtained from Dharmacon (Lafayette, CO, USA). ON-TARGETplus Non-targeting Pool was used as negative control. 0.5×10^5 cells were seeded per well in a 24 multi-well plate and, after 24h and 70% confluence, the siRNA molecules (final concentration 25 nM) were transfected with 1 μ L of MACSfectin per well according to manufacturer's instructions. Forty-eight and 96h after seeding and transfecting the first time, cells were re-plated and re-transfected with the same conditions. The knockdown efficiency was examined by flow cytometry 144h after transfection with the siRNA, and cell proliferation/cell death analyzed as described below.

Flow cytometry-based analyses

To determine whether depletion of candidates had an effect on specific cellular functions, different analyses were performed. For cell cycle analysis, cells were fixed with 4% paraformaldehyde (PFA) 20min and stained with 1 μ g/mL DAPI in a 0.5% saponin solution for

30min. For apoptosis detection, cells were stained with Annexin V-PE (Miltenyi Biotec) and DAPI, according to manufacturer's instructions. Apoptotic cells are positive for Annexin V whereas DAPI⁺ cells have recently died. For cell proliferation, incorporation of EdU (5-ethynyl-2'-deoxyuridine) during DNA synthesis was measured using Click-iT[®] EdU Flow Cytometry Assay Kit (Life Technologies), following manufacturer's instructions. Briefly, cells were incubated with 10 μ M EdU for 2h, collected and washed with 1% BSA in PBS, fixed with 4% PFA 15min, permeabilized with saponin-based buffer 15min, stained with the Click-iT reaction cocktail (containing CuSO₄ and Alexa Fluor[®] 647 azide) for 30min and stained with 1 μ g/mL DAPI. Analysis was performed using the MACSQuant[™] Analyzer and data analysis by MACSQuatify[™] software (Miltenyi Biotec).

Induction and detection of specific stress conditions

To determine how specific stress conditions might affect cell growth, as well as the level of expression of candidate markers, aneuploid cells were exposed to serum-starvation, glucose-deprivation, high confluency, oxidative stress (H₂O₂), or ER stress (Brefeldin, BFA; Thapsigargin, Thps; or Tunicamycin, TM). For this set of experiments, HCT116 18/3 (clones 1 and 2), HCT116 21/3 (clones 1 and 3) and HPT1 cell lines were used, together with HCT116 parental cell line as control.

To determine the effect of growth under high confluence, each cell line was plated in a 6-well plate at a density of 2x10⁵ cells per well and re-plated every 3 days (control) or 6 days (confluent) for 18 days. For the remaining stress conditions, cells were plated in a 6-well plate at a density of 2x10⁵ cells per well and, after 24h, the medium was replaced by standard culture medium without FBS (serum-free) or without glucose (glucose-free), or treated with 100 μ M H₂O₂, 1 μ g/mL BFA, 0.25 μ g/mL Thps or 2.5 μ g/mL TM (all purchased from Sigma-Aldrich), for 2-3 days. After treatment, cells were collected and stained with Abs for the specific markers selected, at a dilution 1:10 at 2-8°C for 10 min, followed by 2 washing steps with PEB.

For oxidative stress detection, the CellROX[®] Deep Red Reagent (Life Technologies) was used to evaluate the levels of reactive oxygen species (ROS) by flow cytometry. For this purpose, the medium was removed from each well and cells were re-incubated with CellROX[®] Reagent at a final concentration of 5 μ M, 30min at 37°C, before analysis. For ER detection, cells were stained 30min with anti-PDI PE antibody (clone 1D3, 1:100, Abcam, Cambridge,

UK), after fixation with 4% PFA 15min RT and permeabilization with saponin-based buffer 15min RT.

Statistical analysis

All statistics and final plots were obtained using GraphPad Prism 6 software and all statistically evaluated experiments were performed in three replicates from at least two independent experiments.

Results

Identification of differentially expressed cell surface markers in aneuploid cells

Two adherent parental cell lines, RPE1 and HCT116, were used to generate cells with an aneuploid karyotype by transferring an additional chromosome via microcell-mediated chromosome transfer (to induce trisomy of chromosome 5, 12, 21 or others), or by inhibiting cytokinesis to generate more complex karyotypes (post-tetraploidy) (7,17) (for more details see Material and Methods). To identify cell surface molecules differentially expressed as compared to the parental cell lines, all cells were analyzed by flow cytometry using a cell surface marker screening panel containing antibodies specific for 291 surface proteins. Two sets of aneuploid cell lines, including three cell lines generated from the RPE1 parental line (RPE1 5/3 12/3, RPE1 21/3 and RPT1) and two from HCT116 parental line (HCT116 5/3 and HCT1), were initially screened with the complete panel of antibodies. Figure 1A-C shows the gating strategy used for the simultaneous analysis of 4 cell lines – 3 aneuploid plus one parental cell line - as well as the read-out of the analysis showing the expression levels for each marker (Figure 1D-I). To detect cell surface markers related to aneuploidy, the trisomic/post-tetraploid cell lines were compared to the corresponding parental cell line and all the markers that were differentially regulated were selected for further validation (Supplementary Figure S1). We measured the mean fluorescence intensity and percentage of positive cells for each surface marker staining across different cell lines (Supplementary Table S4). Analysis of the expression pattern showed 72/291 proteins with altered levels of expression in at least two of the aneuploid karyotypes when compared to the control (HCT116 and RPE1 parental cells); 20 and 18 of the 72 markers were altered in terms of mean intensity value and/or percentage of positive cells in five and four of the screened aneuploid cell lines, respectively. Based on these results, a new 49-marker panel (with additional 5 isotype control antibodies) with the most important candidates was developed for further analyses (Supplementary Table S2).

Validation of candidate markers in independent cell lines

In order to validate the most relevant candidates identified in the two initial high-throughput screenings, 25 additional aneuploid cell lines with different karyotypes were analyzed (e.g. trisomy of chromosome 3, 8, 13 and 18) with the 49-marker panel. In addition, 5 post-

tetraploid cell lines generated from the DLD1 parental cell line were also included (Table 1). For the majority of the clones analyzed in this study, at least two repetitive screenings were performed, with a total of 74 analyses for a total 35 aneuploid cell lines. Surface marker analysis revealed CD230 (PrP, prion protein) as the most frequently increased marker in aneuploid cells compared with the corresponding parental cells (66/74 analysis and 27/35 aneuploid clones). In addition, aneuploid cells showed upregulation of several other markers, including the CD58 cell adhesion molecule (56/74 analyses and 24/35 aneuploid clones), the CUB domain-containing protein CD318 (55/74 analyses and 26/35 aneuploid clones), the Na⁺/K⁺-ATPase subunit CD298 (52/74 analyses and 23/35 aneuploid clones), the HLA-Bw6 molecule (50/74 analyses and 23/35 aneuploid clones), the CD73/ecto-5'-nucleotidase (50/74 analyses and 22/35 aneuploid clones), the CD156c/ADAM10 protein (49/74 analyses and 21/35 aneuploid clones), the complement regulatory proteins CD46 and CD55 (49/74 and 48/74 analyses and 21/35 and 22/35 aneuploid clones, respectively), the CD99 cell adhesion molecule (48/74 analyses and 24/35 aneuploid clones), and CD147/basigin (48/74 analyses and 23/35 aneuploid clones), as well as several members of the integrin family of proteins - CD29 (61/74 analyses and 26/35 aneuploid clones), CD49b (56/74 analyses and 29/35 aneuploid clones), CD47 (52/74 analyses and 26/35 aneuploid clones), CD49f (51/74 analyses and 25/35 aneuploid clones) and CD104 (51/74 analyses and 24/35 aneuploid clones) - (Figure 2A). Of note, CD54/ICAM1 was the most frequently downregulated marker, with lower expression levels detected in 43/74 analyses and 21/35 aneuploid clones. Mean fluorescence intensity data and percentage of positive cells, normalized to the correspondent parental cell line, for all the clones and screenings are available in Supplementary Table S5.

We next asked whether the changes in surface proteome correlate with the identity of the extra chromosome. Unsupervised hierarchical clustering revealed that most clones with the same extra chromosome cluster together, although there is certain heterogeneity, most likely due to clonal effects as each cell line arose from a single cell (Supplementary Figure S2). Importantly, comparison of different cell lines with the clones with the same trisomy showed that only a very few proteins were directly associated with the corresponding aneuploid chromosome. For example, the four clones with trisomy of chromosome 3 (i.e. RPE1 3/3 cl1 and cl2 and HCT116 3/3 cl11 and cl13) all showed overexpression of CD318, with corresponding gene located on 3p21.31, and the clones with trisomy/tetrasomy of the

chromosome 5 (i.e. RPE1 5/3 cl3 and cl7 and HCT116 5/3 and 5/4) showed increased expression of the integrins CD49a and CD49b, coded on chromosome 5. However, CD318 and both integrins were also upregulated in aneuploid cells that contain independent chromosomal amplifications. This indicates that there is only a minor role for chromosomal location and that the upregulated markers represent rather a response to aneuploidy *per se*. Taken together, we have identified 15 markers which are expressed at higher levels in human aneuploid cells than in the corresponding diploids in at least 60% of all analyzed lines. The elevated expression was independent of the cell line, the identity of the extra chromosome or the origin of aneuploidy.

As marker detection by multiparameter flow cytometry was performed at the cell surface level, we used previously published proteome data (7) to confirm whether the expression difference reflects an increased expression or rather an altered localization at the cellular membrane. The available data characterized the proteome from trisomies of chromosome 3 (HCT116 3/3), chromosome 5 (HCT116 H2B-GFP 5/3 and RPE-1 5/3) or chromosome 21 (RPE-1 21/3), and tetrasomy of chromosome 5 (HCT116 5/4 and HCT116 H2B-GFP 5/4). The previously measured aneuploid-to-diploid ratios of protein abundance were compared with the relative changes of the surface proteins determined by flow cytometry (Supplementary Table S6). These data confirmed an increased abundance of most of the candidates, including increased expression of CD230 (PRNP), CD73 (NT5E), CD318 (CDCP1), CD298 (ATP1B3), as well as the CD49b, CD29 and CD51 integrins, in at least five of the six aneuploid cell lines compared to their diploid counterparts.

The overexpression of identified biomarkers is reproduced in primary fibroblasts from patients with trisomy syndromes and mouse models of aneuploidy

To determine whether the differential expression of the identified candidate markers was also associated with aneuploidy in primary cases of trisomy syndromes, fibroblasts from patients with Down's (trisomy 21), Edwards' (trisomy 18) and Patau's (trisomy 13) syndromes were analyzed for the 49 surface markers. When compared with normal fibroblasts, patient samples showed overexpression of several markers, such as CD55 (12/12 screenings), CD58 (12/12), CD99 (12/12), CD230 (11/12), CD90 (11/12), CD95 (10/12), CD97 (10/12), CD147 (10/12), CD10 (10/12), CD73 (9/12) and PTK7 (9/12), in at least 5 of the 6 patients (Figure 2B). Of note, similarly as in model aneuploidy cell lines, CD54 was one of the

most frequent markers (8/12 screenings) showing decreased expression in patients' fibroblasts when compared to the normal counterparts.

In more detail, comparisons among aneuploid cell lines and patients' fibroblasts showed an increased expression of CD97, CD276, CD298, CD29, CD147, CD49e, CD49b and HLA-Bw6, as well as decreased expression of CD54 in cell lines with a trisomy of chromosome 13. Cells with trisomy 18 showed a common increased expression of CD55, CD58, CD99 and CD138, in addition to a decreased expression of CD142. On the other hand, trisomy of chromosome 21 showed higher CD119, CD147 and HLA-Bw6 and lower CD54 expression, on both aneuploid cells and patients' fibroblasts.

To further validate the candidate markers in a completely independent model system, we additionally analyzed an *in vivo* mouse breast cancer model of chromosomal instability. We used a previously generated mouse mammary tumor virus (MMTV)-driven, doxycycline-inducible model (21,23), which overexpress *Kras*^{G12D} or both *Mad2* and *Kras*^{G12D}, since the later tumors have been shown to be highly aneuploid (21). To complement our study, we also used mouse tumors overexpressing *Her2* or both *Her2/PLK1* genes (Venkateswaran *et al.*, unpublished). The mammary adenocarcinomas were characterized according to the CN profile, divided into low- (R1 and R15), intermediate- (R16 and R3) and high-aneuploidy (R10) tumors, and were compared to normal mammary gland tissue. Interestingly, several of the proteins showed comparable patterns of expression in the mouse cells as those observed in their human counterparts. Of note, the results showed an overexpression of the ecto-5'-nucleotidase (CD73) in all the mouse adenocarcinomas when compared to normal mammary cells, with higher levels of expression and percentage of positive cells (Figure 3), as well as increased expression of the mouse H-2K^d/2D^d MHC Class I antigens, the CD146 and CD44 cell adhesion molecules and the CD97v2 receptor (Supplementary Table S7). In addition, higher levels of expression were also detected in the high-aneuploidy tumors when compared to the low-aneuploidy ones, for several members of the integrin (i.e. CD29, CD47, CD49f and CD104) and tetraspanin (i.e. CD9, CD63 and CD151) family of proteins (Supplementary Table S7). Taken together, these results strongly indicate that the identified markers are generic and broadly applicable across aneuploid cells in the human and murine settings.

Expression of CD230 and CD73 in aneuploid cells changes in response to cellular stress

To characterize possible roles of the identified markers on aneuploidy, 6 candidates - the major prion protein (CD230), the ecto-5'-nucleotidase (CD73), the CD55 complement regulatory protein, the CD95 Fas receptor and two members of the integrin family of proteins (CD49b and CD47) - were selected for further functional analyses. Depletion of the candidates by siRNA-mediated knockdown showed no major effect on cell proliferation (% EdU⁺ cells) and cell death (%AnnexinV⁺ cells), when compared to the non-targeting siRNA control on both the HCT116 parental and HPT1 cells (Supplementary Figure S3). Therefore, the expression of those markers seems to be non-essential for the cells, at least over limited period of time and under the tested conditions.

We next investigated whether the expression of selected candidates correlates to specific stress conditions known to affect aneuploid cells. Aneuploidy is known to induce cellular stress (24) and recent reports suggest an association between aneuploidy and an advantageous phenotype under stress conditions (3). Aneuploid clones with negative or low expression of the markers (HCT116 18/3 cl2 and 21/3 cl1 and 3) were compared to clones with high levels of expression (HPT1 and HCT116 18/3 cl1), as well as HCT116 parental cells as control. The investigated stress conditions included growth at a high confluency, serum-starvation, glucose-deprivation, oxidative stress and ER stress. To evaluate whether the stress conditions could alter the expression of those candidates, cells were initially grown under high confluency. Results showed a significant increase in the percentage of CD73⁺ cells for both HCT116 21/3 clones ($p < 0.0001$, 0 vs 6, 6 vs 12 and 12 vs 18 days) compared to parental cells ($p < 0.0001$, 0 vs 6 days) (Figure 4A). Of note, parental cells showed only a slight initial increase in the percentage of CD73⁺ cells, which stabilized over the time period of the experiment (Figure 4A and B). This indicates that the stress response and corresponding CD73 expression is significantly increased in aneuploid setting.

We next analyzed whether cells with different degrees of aneuploidy show correlating levels of ER or oxidative stress. Whereas no significant differences were found for clones with only one extra chromosome, near-tetraploid clones, associated with higher levels of aneuploidy, showed higher expression of the ER stress marker protein disulfide isomerase (PDI), as well as higher reactive oxygen species (ROS), when compared to parental cells ($p < 0.01$; Figure 5A and B). To further evaluate the impact of ER stress on aneuploid cells, we determined the

effect of glucose-deprivation, 1 μ g/mL brefeldin A, 0.25 μ g/ml thapsigargin or 2.5 μ g/mL tunicamycin on the expression levels of the candidates. However, results suggested a general decrease for mean fluorescence intensity of the cell surface markers, as the treatment probably blocked the assembly of new proteins in the ER and/or the transport of proteins from the ER to the cell surface (Supplementary Figure S4). To test the effect of oxidative stress, we treated cells with 100 μ M H₂O₂, a commonly used method to induce oxidative stress in cells (25). We observed a general increase for all analyzed proteins, most particularly for the CD95 FAS receptor, possibly due to the high toxicity of the treatment (Supplementary Figure S5).

In addition, we tested the response of cells to 3 days of FBS-starvation as an alternative approach to induce oxidative stress with lower toxic effects (26). Indeed, the results revealed that serum-starvation (0% FBS), but not glucose-deprivation increased the generation of ROS in both parental and aneuploid cells ($p < 0.01$ vs cells growing under 10% FBS; Figure 5C). The increased ROS resulted in an increase in the mean fluorescence intensity and/or percentage of positive cells of CD73, CD49b, CD95, and CD230, with CD230 showing the most significant increase (Figure 5D). Furthermore, all clones showing an intermediate expression of CD230 became CD230 positive (HCT116 18/3 cl2, HCT116 21/3 cl1 and 3, as well as HCT116 wild-type), while those clones already expressing CD230 (HPT1 and HCT116 18/3 cl2) showed a significant increase in the mean intensity level ($p < 0.001$ vs 10% FBS control cells; Figure 5D and Supplementary Figure S6). These results suggest that serum-starvation increases the expression of CD230 in response to increased oxidative stress. Subsequent depletion of CD230 by siRNA-mediated knockdown followed by 3 days of FBS-starvation showed no significant effect on cell proliferation (data not shown), but a significant increase in the percentage of necrotic DAPI⁺ HPT1 aneuploid cells compared to the non-targeting siRNA control ($p < 0.001$; Figure 5E). A slight, but not significant increase of necrosis as well as elevated percentage of apoptotic (Annexin V⁺) cells was also detected in HCT116 parental cells. These results confirm an important role of CD230 in cell survival upon oxidative stress, which is further emphasized in cells already compromised by aneuploidy.

Taken together, our data indicate that overexpression of the identified cell surface markers, particularly CD230 and CD73, is correlated to cellular stress, which is increased in cells with aneuploid chromosome settings and might confer survival advantages under stress conditions.

Discussion

The possible impact of aneuploidy on human health has been recognized for over a century, but its effects at the cellular level, such as the specific phenotype arising from aneuploidy, have only become a focus in more recent studies (2). Moreover, transcriptome and proteome analysis revealed common expression changes, suggesting the possibility that some of these changes might be used as markers of aneuploidy. In the present study, we applied a novel cell surface marker screening analysis to evaluate the expression pattern of 291 proteins in order to identify biomarkers related to aneuploidy. Using this strategy we aimed not only to determine surface marker candidates, which would allow to detect and/or quantify aneuploidy in tumors, but also to provide insights into the underlying mechanisms that allow the cells with aneuploid karyotypes to grow despite the detrimental effects of aneuploidy on cellular physiology. To ensure a broad coverage of aneuploidy types, cells with one or two extra chromosomes (7), near-tetraploid karyotypes (17), embryo- and patient-derived cell lines with trisomy syndromes, as well as mouse models of aneuploidy (14) were all included in this study and screened for their surface proteome.

Using this approach, we identified several proteins upregulated in aneuploid cells when compared to the corresponding diploid parental cells. Remarkably, the strongest candidates included proteins which have been previously associated with cancer, namely the prion protein (PrP^C, CD230) (27), the ecto-5'-nucleotidase (ecto-5'-NT, CD73) (28), the CUB domain-containing protein CD318 (29), the Na⁺/K⁺-ATPase subunit CD298 (30), the disintegrin-metalloproteinase ADAM10 (CD156c) (31), the complement regulatory proteins CD46 and CD55 (32), the CD58 and CD99 cell adhesion molecules, the basigin (CD147) (33), as well as several members of the integrin family of proteins, e.g. CD29, CD49b, CD47, CD49f and CD104, which are expressed by tumor and tumor-associated host cells to mediate a diverse array of cellular effects resulting in tumor progression and metastasis (34). Interestingly, expression of several of these markers, such as CD230, CD73, CD55, CD58, CD99, was also elevated in primary fibroblasts from patients with Down's (trisomy 21), Edwards' (trisomy 18) and Patau's (trisomy 13) syndromes when compared to normal fibroblasts, thus suggesting a possible role for these proteins in aneuploid settings independent of cancer.

Using mouse models of aneuploidy, we further found that aneuploid mouse breast tumor cells also overexpress several of the identified candidate proteins such as the CD73 enzyme and multiple members of the integrin family of proteins. Interestingly, while the ecto-5'-NT enzyme was absent on both normal mammary gland cells as well as in non-tumoral lineages, all aneuploid tumors derived from four different mouse models (*Kras*^{G12D}, *Kras*^{G12D}/*Mad2*, *Her2*, and *Her2/PLK1*) harbored a subpopulation of tumor cells defined by the expression of this marker that ranged from 30% to 100 % of the tumor. Moreover, the expression levels often scaled with the degree of aneuploidy: the most aneuploid tumor (R10) showed the highest levels of CD73 expression while tumors with lower CNV showed only intermediate expression of CD73 in comparison to diploid cells. Of note, it is important to consider that not all the antibodies had a mouse specific counterpart (29 mouse/49 human specific Abs), thereby the expression intensity of some of the markers could not be validated in the respective mouse models.

When taking all used models into account, two markers - PrP^C and ecto-5'-NT - particularly stand out due to their low or absent expression in diploid cells, while the majority of the aneuploid cells showed a positive subpopulation, with variable percentages among the different clones and models (Figure 1F and I). PrP is well known for its role in the pathogenesis and transmission of prion diseases. Despite the abundant information on the function of the misfolded prion protein (PrP^{Sc}), the function of the cellular prion protein (PrP^C) remains largely unknown (27). However, multiple reports have suggested a putative role for PrP^C in cell signaling, survival, and differentiation (27,35,36) and, more recently, a large body of evidence suggests that PrP^C is overexpressed in different types of cancers and its expression appears to be associated with poor prognosis and resistance to therapy (37-41). Similarly, the ecto-5'-NT/CD73, a membrane-bound enzyme that catalyzes the hydrolysis of AMP into adenosine and phosphate, has also been found to be overexpressed in many types of cancer (28), with multiple key roles in tumor development. CD73 can act as a signal and adhesive molecule that regulates cell interaction with extracellular matrix components (e.g. laminin and fibronectin) to mediate cancer invasiveness and metastatic properties, as well as playing a key important role in the tumor immunoescape due to CD73-generated adenosine (42). In line with such evidences, our results suggest that increased surface abundance of these proteins may contribute to the phenotypic changes observed in aneuploid cells.

It is currently known that the aneuploid state of the cell elicits several cellular stress responses such as proteotoxic (24,43) and oxidative stresses (44). How these “aneuploidy-associated stresses” affect cells and how cells respond to them are not yet clear (24,43). The possibility that aneuploidy triggers such stress responses in order to adapt and proliferate with their altered genomes has been recently proposed (24). In fact, evidences show that the effects of aneuploidy may become advantageous under environmental stress, most possibly due to the karyotypic/phenotypic heterogeneity arising in aneuploid cell populations caused by chromosomal instability, which ultimately provides superior adaptability and a growth advantage under selective conditions (24,45). Based on this, and due to the lack of an effect of marker-depletion on cell proliferation and cell death (apoptosis), we hypothesize that the expression of the marker candidates may be related to cellular stress. Indeed, our results showed that high levels of aneuploidy (i.e. the near-tetraploid clones) were correlated with higher levels of both ER and oxidative stress. Most strikingly, clones with an extra copy of chromosome 21, which were initially negative for CD73, strongly increased the expression of CD73⁺ cells when grown under high confluency, while parental diploid cells only slightly increased expression early on and stabilized over time. A high confluency environment most certainly leads to hypoxia, a condition known to promote selection of resistant, aggressive cancer cells able to survive in unfavorable environments, with greater proliferative and migratory capacity (46). Accordingly, CD73 expression can be driven by an hypoxic microenvironment as the CD73 gene promoter has at least one binding site for the hypoxia-inducible factor-1 α (42,47) in order to convert AMP to adenosine and, consequently, to enhance tumor survival (46). Thus, we hypothesize that aneuploid cells might overexpress the ecto-5'-NT enzyme as a mechanism to gain protection under specific conditions and to support proliferation. In addition, under serum-free conditions both parental and aneuploid cells highly increased the expression of PrP^C, as well as the generation of ROS, indicating that the higher levels of PrP^C expressed by aneuploid cells (compared to normal cells) can probably confer an advantage against oxidative stress. Indeed, we found that aneuploid cells showed increased cell death under serum starvation after depletion of PrP^C. These results are consistent with one of the emerging functions reported for PrP^C, its protective role for cell survival, including protection against oxidative stress and serum deprivation (36), as well as hypoxia (48). In addition, PrP^C has been described as an important modulator of tumor growth via engagement to the ligand

HSP70/90 heat shock organizing protein (49). Interestingly, Bravard *et al.* (50) also reported recently a key role of PrP^C in the DNA damage response, suggesting that PrP^C is required to maintain genomic stability in response to genotoxic stress. The authors showed that exposure to genotoxic stress activates PRNP transcription and increases the amount of PrP^C in the nucleus, where it stimulates the endonuclease APE1, essential for base excision repair. Such evidences, together with our data, suggest that aneuploid clones might overexpress PrP^C in order to increase protection from oxidative stress as well as DNA damage and, consequently, increase survival of aneuploid clones. Based on these data we propose that the identified changes in surface proteins reflect the cellular response to aneuploidy that is independent of the chromosome composition or the cell type. These proteins likely facilitate growth of aneuploid cells by protecting them from endogenous stresses caused by unbalanced karyotype.

In summary, we have identified multiple cell surface biomarkers with altered expression in aneuploid cells. The most striking and general overexpression was seen for the CD230/PrP^C protein and the enzyme CD73/ecto-5'-NT. Furthermore, we have shown that overexpression of both markers in aneuploid cells is associated to increased cellular stress, which may help to explain how aneuploidy confers a selective advantage to cells. CD230 and CD73 may therefore represent key markers to detect aneuploidy in healthy as well as tumor samples. Further studies to understand the full impact of these markers on aneuploid cells will not only deepen our knowledge on the consequences of an abnormal karyotype, but will also increase our insight into disabilities such as Down's syndrome and diseases such as cancer.

Acknowledgements

We are grateful to Daniela Lehnen, Janina Kuhl and Aline Campos for excellent technical assistance.

References

1. Orr B, Godek KM, Compton D. Aneuploidy. *Curr Biol* **2015**;25:R538-42.
2. Pfau SJ, Amon A. Chromosomal instability and aneuploidy in cancer: from yeast to man. *EMBO Rep* **2012**;13:515-27.
3. Rutledge SD, Douglas TA, Nicholson JM, Vila-Casadesus M, Kantzler CL, Wangsa D, *et al.* Selective advantage of trisomic human cells cultured in non-standard conditions. *Sci Rep* **2016**;6:22828.
4. Holland AJ, Cleveland DW. Losing balance: the origin and impact of aneuploidy in cancer. *EMBO Rep* **2012**;13:501-14.
5. Nowak MA, Komarova NL, Sengupta A, Jallepalli PV, Shih Ie M, Vogelstein B, *et al.* The role of chromosomal instability in tumor initiation. *Proc Natl Acad Sci U S A* **2002**;99:16226-31.
6. Duijf PH, Benezra R. The cancer biology of whole-chromosome instability. *Oncogene* **2013**;32:4727-36.
7. Stinge S, Stoehr G, Peplowska K, Cox J, Mann M, Storchova Z. Global analysis of genome, transcriptome and proteome reveals the response to aneuploidy in human cells. *Mol Syst Biol* **2012**;8:608.
8. Dephore N, Hwang S, O'Sullivan C, Dodgson SE, Gygi SP, Amon A, *et al.* Quantitative proteomic analysis reveals posttranslational responses to aneuploidy in yeast. *Elife* **2014**;3:e03023.
9. Pavelka N, Rancati G, Zhu J, Bradford WD, Saraf A, Florens L, *et al.* Aneuploidy confers quantitative proteome changes and phenotypic variation in budding yeast. *Nature* **2010**;468:321-5.
10. Torres EM, Sokolsky T, Tucker CM, Chan LY, Boselli M, Dunham MJ, *et al.* Effects of aneuploidy on cellular physiology and cell division in haploid yeast. *Science* **2007**;317:916-24.
11. Durrbaum M, Kuznetsova AY, Passerini V, Stinge S, Stoehr G, Storchova Z. Unique features of the transcriptional response to model aneuploidy in human cells. *BMC Genomics* **2014**;15:139.
12. Sheltzer JM, Torres EM, Dunham MJ, Amon A. Transcriptional consequences of aneuploidy. *Proc Natl Acad Sci U S A* **2012**;109:12644-9.
13. Torres EM, Dephore N, Panneerselvam A, Tucker CM, Whittaker CA, Gygi SP, *et al.* Identification of aneuploidy-tolerating mutations. *Cell* **2010**;143:71-83.
14. Schvartzman JM, Sotillo R, Benezra R. Mitotic chromosomal instability and cancer: mouse modelling of the human disease. *Nat Rev Cancer* **2010**;10:102-15.
15. Donnelly N, Storchova Z. Dynamic karyotype, dynamic proteome: buffering the effects of aneuploidy. *Biochim Biophys Acta* **2014**;1843:473-81.
16. Passerini V, Ozeri-Galai E, de Pagter MS, Donnelly N, Schmalbrock S, Kloosterman WP, *et al.* The presence of extra chromosomes leads to genomic instability. *Nat Commun* **2016**;7:10754.
17. Kuznetsova AY, Seget K, Moeller GK, de Pagter MS, de Roos JA, Durrbaum M, *et al.* Chromosomal instability, tolerance of mitotic errors and multidrug resistance are promoted by tetraploidization in human cells. *Cell Cycle* **2015**;14:2810-20.
18. Dewhurst SM, McGranahan N, Burrell RA, Rowan AJ, Gronroos E, Endesfelder D, *et al.* Tolerance of whole-genome doubling propagates chromosomal instability and accelerates cancer genome evolution. *Cancer Discov* **2014**;4:175-85.
19. Drosopoulos K, Tang C, Chao WC, Linardopoulos S. APC/C is an essential regulator of centrosome clustering. *Nat Commun* **2014**;5:3686.
20. Donnelly N, Passerini V, Durrbaum M, Stinge S, Storchova Z. HSF1 deficiency and impaired HSP90-dependent protein folding are hallmarks of aneuploid human cells. *EMBO J* **2014**;33:2374-87.

21. Rowald K, Mantovan M, Passos J, Buccitelli C, Mardin BR, Korbel JO, *et al.* Negative Selection and Chromosome Instability Induced by Mad2 Overexpression Delay Breast Cancer but Facilitate Oncogene-Independent Outgrowth. *Cell Rep* **2016**;15:2679-91.
22. Dunphy KA, Tao L, Jerry DJ. Mammary epithelial transplant procedure. *J Vis Exp* **2010**
23. Sotillo R, Hernando E, Diaz-Rodriguez E, Teruya-Feldstein J, Cordon-Cardo C, Lowe SW, *et al.* Mad2 overexpression promotes aneuploidy and tumorigenesis in mice. *Cancer Cell* **2007**;11:9-23.
24. Santaguida S, Amon A. Short- and long-term effects of chromosome mis-segregation and aneuploidy. *Nat Rev Mol Cell Biol* **2015**;16:473-85.
25. Coyle CH, Kader KN. Mechanisms of H₂O₂-induced oxidative stress in endothelial cells exposed to physiologic shear stress. *ASAIO J* **2007**;53:17-22.
26. Pandey S, Lopez C, Jammu A. Oxidative stress and activation of proteasome protease during serum deprivation-induced apoptosis in rat hepatoma cells; inhibition of cell death by melatonin. *Apoptosis* **2003**;8:497-508.
27. Mehrpour M, Codogno P. Prion protein: From physiology to cancer biology. *Cancer Lett* **2010**;290:1-23.
28. Gao ZW, Dong K, Zhang HZ. The roles of CD73 in cancer. *Biomed Res Int* **2014**;2014:460654.
29. Wortmann A, He Y, Deryugina EI, Quigley JP, Hooper JD. The cell surface glycoprotein CD147 in cancer--insights, opportunities, and challenges. *IUBMB Life* **2009**;61:723-30.
30. Mijatovic T, Dufresne F, Kiss R. Na⁺/K⁺-ATPase and cancer. *Pharm Pat Anal* **2012**;1:91-106.
31. Moss ML, Stoeck A, Yan W, Dempsey PJ. ADAM10 as a target for anti-cancer therapy. *Curr Pharm Biotechnol* **2008**;9:2-8.
32. Mamidi S, Hone S, Kirschfink M. The complement system in cancer: Ambivalence between tumour destruction and promotion. *Immunobiology* **2015**
33. Muramatsu T. Basigin (CD147), a multifunctional transmembrane glycoprotein with various binding partners. *J Biochem* **2016**;159:481-90.
34. Desgrosellier JS, Cheresch DA. Integrins in cancer: biological implications and therapeutic opportunities. *Nat Rev Cancer* **2010**;10:9-22.
35. Roucou X, Giannopoulos PN, Zhang Y, Jodoin J, Goodyer CG, LeBlanc A. Cellular prion protein inhibits proapoptotic Bax conformational change in human neurons and in breast carcinoma MCF-7 cells. *Cell Death Differ* **2005**;12:783-95.
36. Vassallo N, Herms J, Behrens C, Krebs B, Saeki K, Onodera T, *et al.* Activation of phosphatidylinositol 3-kinase by cellular prion protein and its role in cell survival. *Biochem Biophys Res Commun* **2005**;332:75-82.
37. Meslin F, Hamai A, Gao P, Jalil A, Cahuzac N, Chouaib S, *et al.* Silencing of prion protein sensitizes breast adriamycin-resistant carcinoma cells to TRAIL-mediated cell death. *Cancer Res* **2007**;67:10910-9.
38. Du J, Pan Y, Shi Y, Guo C, Jin X, Sun L, *et al.* Overexpression and significance of prion protein in gastric cancer and multidrug-resistant gastric carcinoma cell line SGC7901/ADR. *Int J Cancer* **2005**;113:213-20.
39. Lopes MH, Santos TG, Rodrigues BR, Queiroz-Hazarbassanov N, Cunha IW, Wasilewska-Sampaio AP, *et al.* Disruption of prion protein-HOP engagement impairs glioblastoma growth and cognitive decline and improves overall survival. *Oncogene* **2015**;34:3305-14.
40. Chieng CK, Say YH. Cellular prion protein contributes to LS 174T colon cancer cell carcinogenesis by increasing invasiveness and resistance against doxorubicin-induced apoptosis. *Tumour Biol* **2015**;36:8107-20.
41. Cheng Y, Tao L, Xu J, Li Q, Yu J, Jin Y, *et al.* CD44/cellular prion protein interact in multidrug resistant breast cancer cells and correlate with responses to neoadjuvant chemotherapy in breast cancer patients. *Mol Carcinog* **2014**;53:686-97.
42. Allard B, Turcotte M, Stagg J. CD73-generated adenosine: orchestrating the tumor-stroma interplay to promote cancer growth. *J Biomed Biotechnol* **2012**;2012:485156.

43. Santaguida S, Vasile E, White E, Amon A. Aneuploidy-induced cellular stresses limit autophagic degradation. *Genes Dev* **2015**;29:2010-21.
44. Li M, Fang X, Baker DJ, Guo L, Gao X, Wei Z, *et al.* The ATM-p53 pathway suppresses aneuploidy-induced tumorigenesis. *Proc Natl Acad Sci U S A* **2010**;107:14188-93.
45. Chen G, Mulla WA, Kucharavy A, Tsai HJ, Rubinstein B, Konkright J, *et al.* Targeting the adaptability of heterogeneous aneuploids. *Cell* **2015**;160:771-84.
46. Young A, Mittal D, Stagg J, Smyth MJ. Targeting cancer-derived adenosine: new therapeutic approaches. *Cancer Discov* **2014**;4:879-88.
47. Synnestvedt K, Furuta GT, Comerford KM, Louis N, Karhausen J, Eltzschig HK, *et al.* Ecto-5'-nucleotidase (CD73) regulation by hypoxia-inducible factor-1 mediates permeability changes in intestinal epithelia. *J Clin Invest* **2002**;110:993-1002.
48. Guitart K, Loers G, Buck F, Bork U, Schachner M, Kleene R. Improvement of neuronal cell survival by astrocyte-derived exosomes under hypoxic and ischemic conditions depends on prion protein. *Glia* **2016**;64:896-910.
49. de Lacerda TC, Costa-Silva B, Giudice FS, Dias MV, de Oliveira GP, Teixeira BL, *et al.* Prion protein binding to HOP modulates the migration and invasion of colorectal cancer cells. *Clinical & experimental metastasis* **2016**;33:441-51.
50. Bravard A, Auvre F, Fantini D, Bernardino-Sgherri J, Sissoeff L, Daynac M, *et al.* The prion protein is critical for DNA repair and cell survival after genotoxic stress. *Nucleic Acids Res* **2015**;43:904-16.

Table 1. Overview of cell lines included in the study, with corresponding karyotype and clones.

Parental cell line	Karyotype	Clones	H2B-GFP	Origin
HCT116	3/3	11, 13	+	Passerini <i>et al.</i> 2016 (16); Stingele <i>et al.</i> 2012 (7)
	5/3	ns	+	Passerini <i>et al.</i> 2016 (16); Stingele <i>et al.</i> 2012 (7)
	5/4	ns	+	Passerini <i>et al.</i> 2016 (16); Stingele <i>et al.</i> 2012 (7); Dürrbaum <i>et al.</i> 2014 (11)
	8/3	3, 5, 7	+	Donnelly <i>et al.</i> , 2014 (20)
	13/3	2, 3	-	This study
	18/3	1, 2	-	This study
	21/3	1, 3	-	This study
	5/3 3/3	ns	-	This study
	Near-4N (HPT)	1, 2, 4	+	Kuznetsova <i>et al.</i> 2015 (17); Dürrbaum <i>et al.</i> 2014 (11)
	Near-4N (TC) ^a	4, 13, 17	-	Dewhurst <i>et al.</i> 2014 (18)
RPE-1 hTERT	3/3	1, 2	-, +	Stingele <i>et al.</i> 2012 (7)
	5/3	3, 7	-	This study
	12/3	ns	-	This study
	21/3	ns	+	Passerini <i>et al.</i> 2016 (16); Stingele <i>et al.</i> 2012 (7); Dürrbaum <i>et al.</i> 2014 (11)
	5/3 12/3	ns	-	Passerini <i>et al.</i> 2016 (16); Stingele <i>et al.</i> 2012 (7); Dürrbaum <i>et al.</i> 2014 (11)
	Near-4N (RPT)	1, 3, 4	+	Kuznetsova <i>et al.</i> 2015 (17)
DLD1	Near-3N	7, 13, 16	-	Viganó <i>et al.</i> in preparation
	4N	ns	-	Drosopoulos <i>et al.</i> 2014 (19)
	>4N	ns	-	Viganó <i>et al.</i> in preparation
Patients with trisomy syndromes	Patau's (13/3)	1 ^b	-	Coriell Institute No. AG10292
	Edwards' (18/3)	2 ^b	-	Coriell Institute No. AG12614 and GM03538
	Down's (21/3)	3 ^b	-	Coriell Institute No. GM01137A, GM02767D and AG06872A

Karyotype nomenclature: 3/3, 5/3, 8/3, 12/3, 13/3, 18/3 and 21/3, trisomy of chromosome 3, 5, 8, 12, 13, 18 and 21, respectively; 5/4, tetrasomy of chromosome 5; HPT, post-tetraploid generated from HCT116; TC, Tetraploid clone; RPT, post-tetraploid generated from RPE1. All the aneuploid cell lines generated from HCT116 and RPE1 were, unless otherwise indicated (^a), developed at the Max Planck Institute of Biochemistry (Martinsried, Germany), and the DLD1-derived lines developed at the Biozentrum - University of Basel (Basel, Switzerland); (^a) cell lines generated at the Francis Crick Institute (London, United Kingdom). (^b) Number of cell lines used in the study are specified, instead of the ID of the clone. Fibroblasts from patients with trisomy syndromes were purchased from the Coriell Institute (Camden, New Jersey, USA). (ns) Clone number not specified.

Figure legends

Figure 1. Representative gating strategy and read-out for analysis of cell surface marker expression.

Cells are first gated in a FSC-A vs SSC-A plot to exclude debris **(A)**, followed by doublet exclusion on a FSC-A vs FSC-H plot (not shown) and dead cell exclusion on a PE-A vs PI-A plot **(B)**. The cell lines included in the screening were then individually gated on a plot FITC-A (H2B-GFP⁺ or CFSE⁺ cells) vs VioBlue-A (VioDye⁺ cells) **(C)** for independent analysis of both percentage of positive cells and median fluoresce intensity levels **(D-I)**; representative expression patterns of relevant candidates are shown. In the represented screening, four individual cell lines were included with H2B-GFP⁻/VioDye⁻ (HCT116 parental cell line, black gate), H2B-GFP⁺/VioDye⁻ (HPT2 post-tetraploid clone, green gate), H2B-GFP⁻/VioDye⁺ (HCT116 5/3 3/3 trisomies, blue gate) and H2B-GFP⁺/VioDye⁺ (HPT4 post-tetraploid clone, red gate) phenotypes.

Figure 2. Identification of differentially expressed cell surface markers in aneuploid cells.

Frequency of **(A)** aneuploid cell lines (n=74, 35 different aneuploid clones plus replicates) and **(B)** primary fibroblasts from patients with trisomy syndromes (n=12, 6 different patients plus replicates) showing increased or decreased expression of the 49 cell surface markers analyzed, compared to the corresponding parental cell line or diploid fibroblasts, respectively. Red and green bars indicate number of cases with increased and decreased expression, respectively, and each bar represents a different protein. At the bottom, representative Venn diagrams of three aneuploid cell lines (HCT116 5/4, HCT116 8/3 clone3, post-tetraploid HPT1) and three patients with trisomy syndromes are shown, in order to identify commonly upregulated (red) or downregulated (green) markers.

Figure 3. Representative gating strategy for immunophenotypic analysis of mouse tumors.

Cells were first gated in a FSC-A vs SSC-A plot **(A)**, followed by dead cell and doublet exclusion on a PE-A vs PI-A **(B)** and FSC-A vs FSC-H plot **(C)**, respectively. The tumor samples and control tissue (normal mammary gland) included in each screening were then individually gated based on VioBlue-A detection (VioDye⁺ cells) and non-tumor cell (NTC; FITC⁺ or APC⁺ cells) exclusion; R16 tumor sample (dark blue gate; NTC, light blue gate) and a

control (black gate) are represented **(D)**. The level of CD73 expression for the three populations **(E)** and the percentage of CD73⁺ tumor cells **(F)** are shown. **(G-I)** Histograms indicate the level of CD73 expression in all tumor samples analyzed (R1, R4 and R15, red lines; R5, R10 and R3, green lines) compared to normal mammary gland (CTRL, black lines).

Figure 4. CD73 expression is increased in aneuploid cells growing under high confluency

(A) The graphs show the percentage of CD73⁺ cells in HCT116 and two trisomy 21 clones growing under normal conditions (dotted line) or under high confluency (solid line) for 18 days. Data are reported as mean and standard deviations for three replicates from two independent experiments. Statistical analysis was performed using the two-way ANOVA to compare differences between groups per each time point. (*) represents time points which showed statistically a significant difference compared to the previous time point ($p < 0.0001$). **(B)** Representative dotplots of FSC-A vs %CD73⁺ cells for control and confluent cells at day 18 are shown, for HCT116 parental cells (top plots), HCT116 21/3 cl1 (center plots) and HCT116 21/3 cl3 (bottom plots).

Figure 5. Oxidative and ER stress in aneuploid cells and its effect on CD73, CD230, CD49b and CD95 expression and cell death.

Higher levels of aneuploidy correlate with higher expression of protein disulfide isomerase (PDI), an ER stress marker **(A)**, as well as higher reactive oxygen species (ROS), as shown by the CellROX fluorescent ROS indicator. Aneuploid clones show higher generation of ROS after treated with 100 μ M H₂O₂ 18h (grey bars) compared to parental cells **(B)**. Serum-starvation (0% FBS; grey bars) for 3 days, rather than glucose-deprivation (white bars), increased the generation of ROS **(C)**, with correlating increased expression of CD230, CD73, CD49b and CD95 in at least one of the cell lines **(D)**. Effect of 3 day-serum starvation after CD230 siRNA knockdown on cell death, analyzed by percentage of apoptotic (AnnexinV⁺) and necrotic (DAPI⁺) cells on HCT116 parental and HPT1 post-tetraploid cell lines **(E)**. Data are reported as mean and standard deviations for three replicates from two independent experiments and statistical analysis was performed using the two-way ANOVA (* $p < 0.01$ and ** $p < 0.0001$).

Figure 1

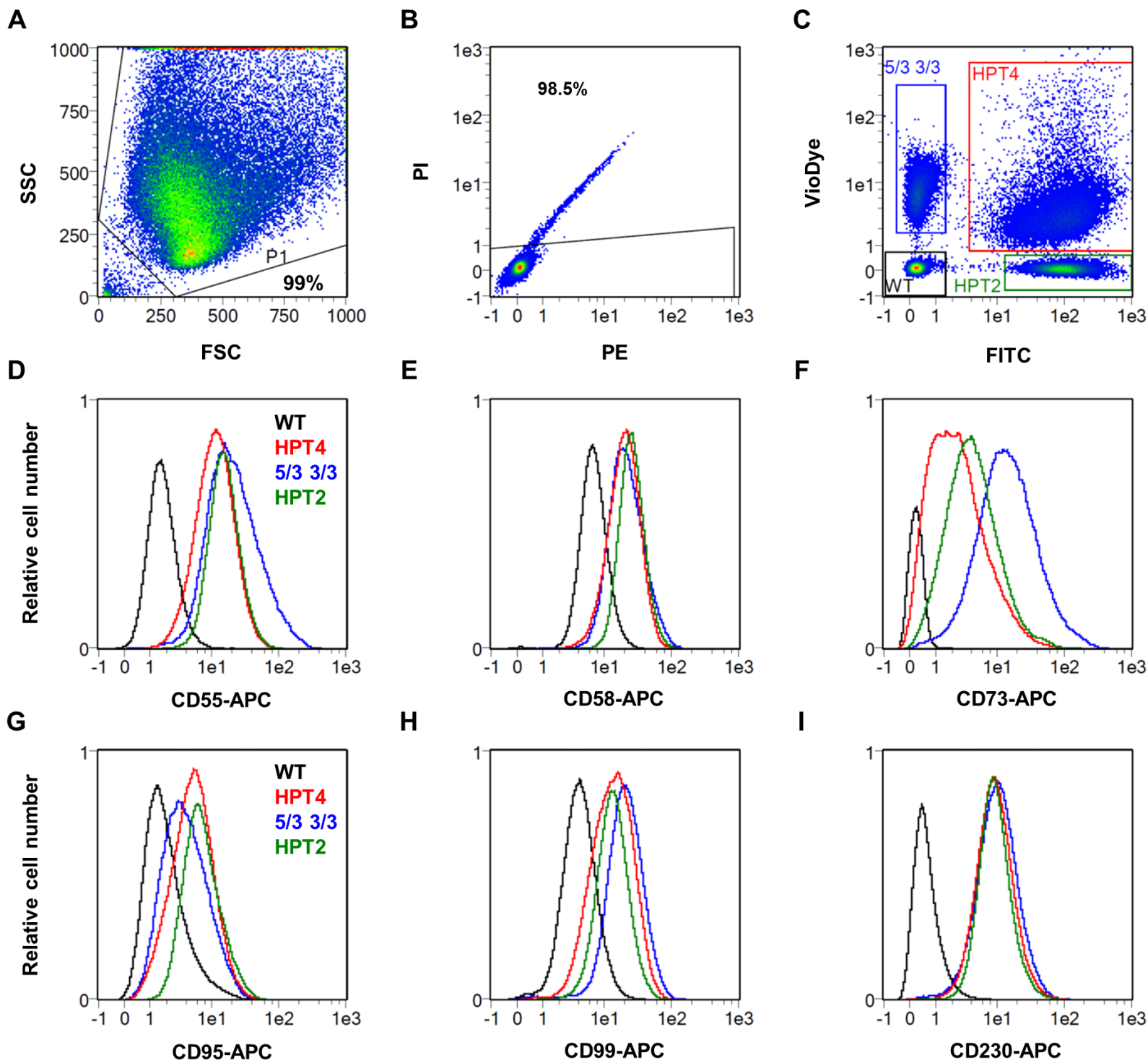


Figure 2

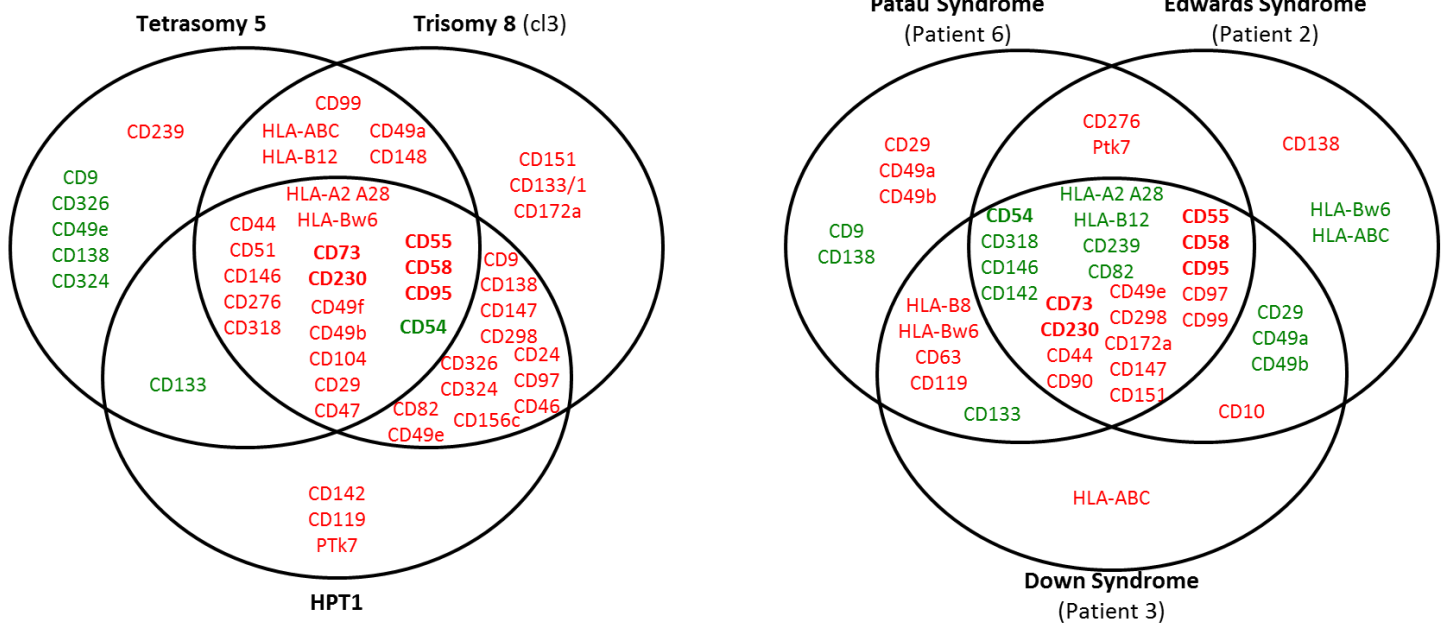
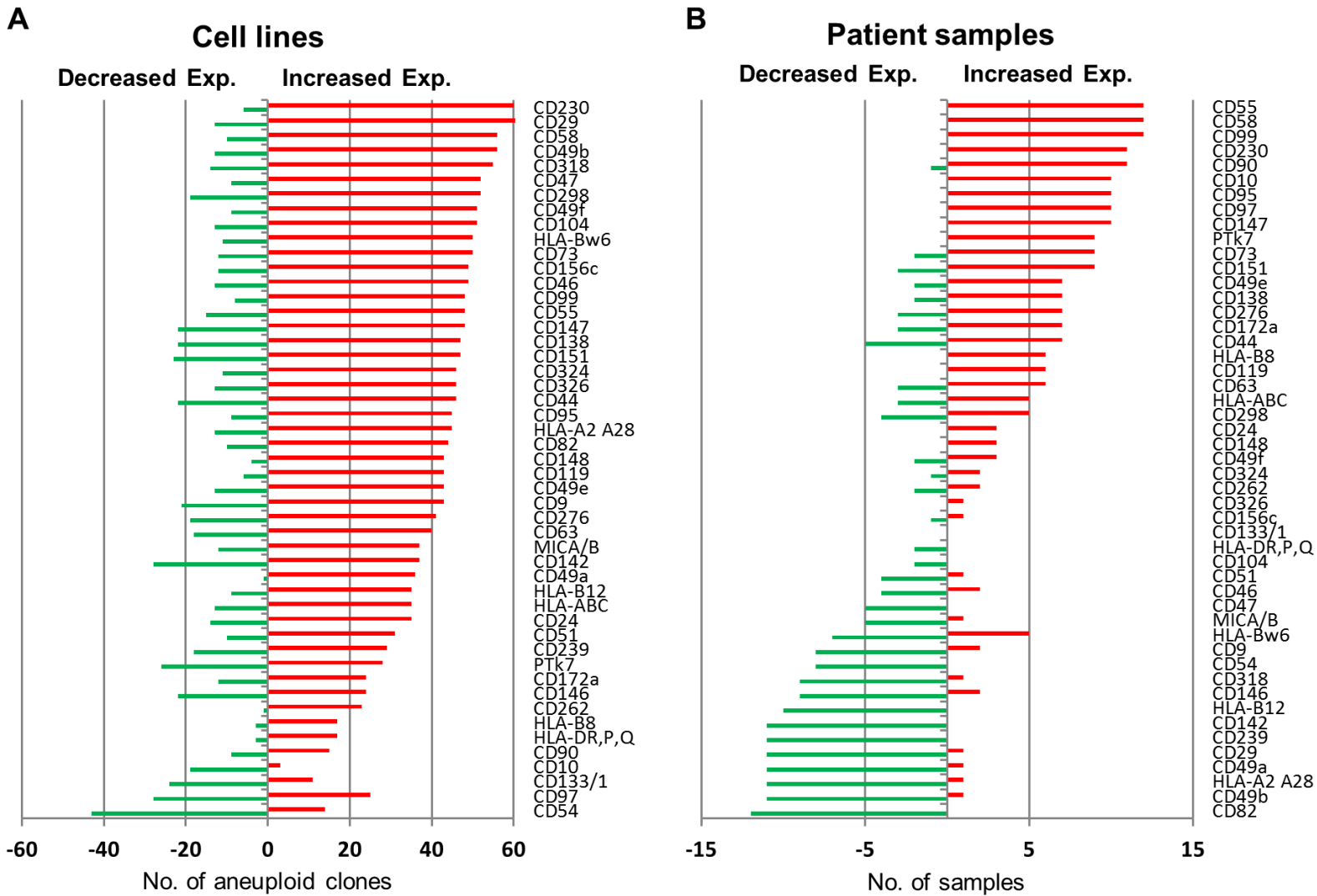


Figure 3

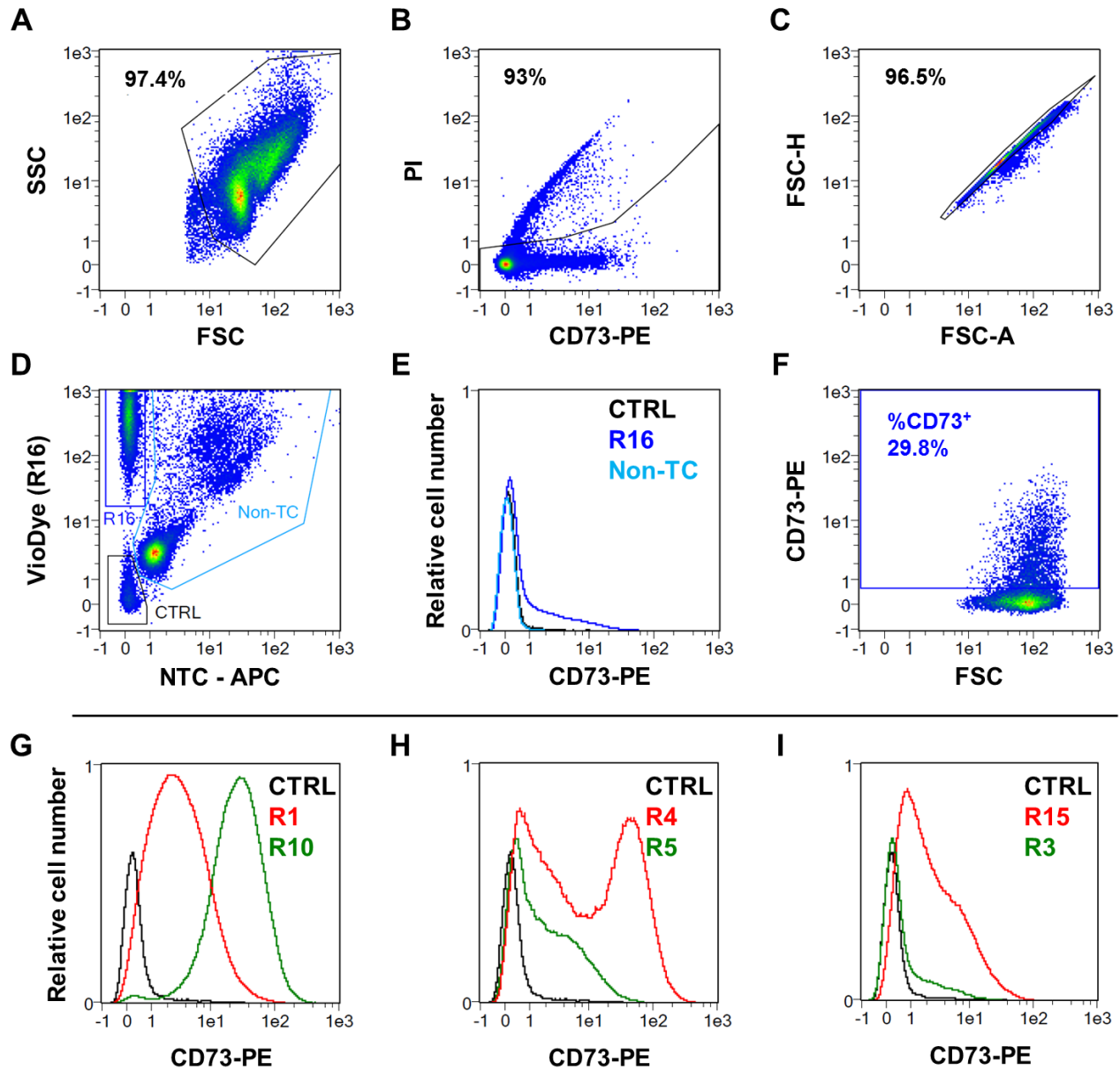


Figure 4

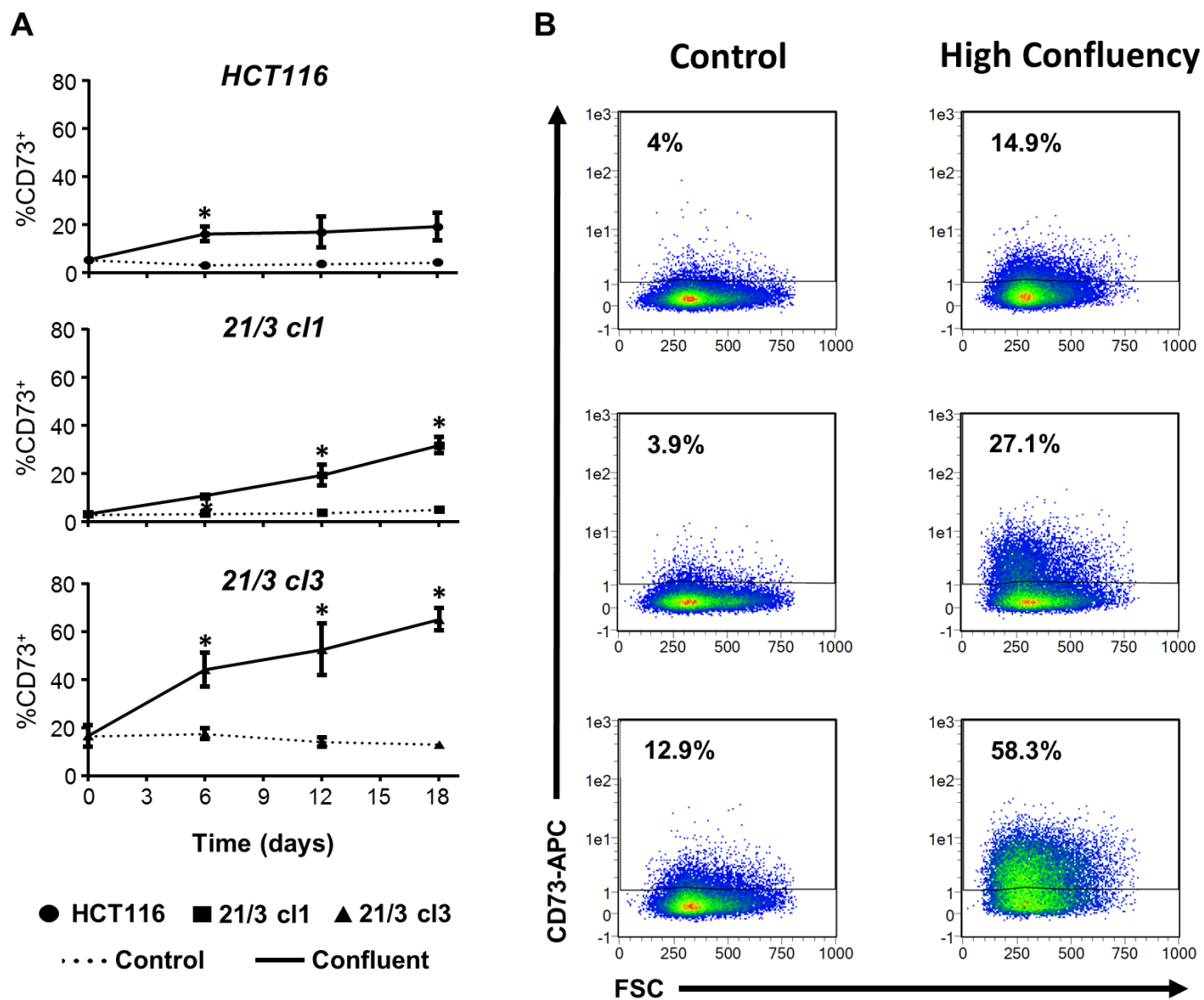
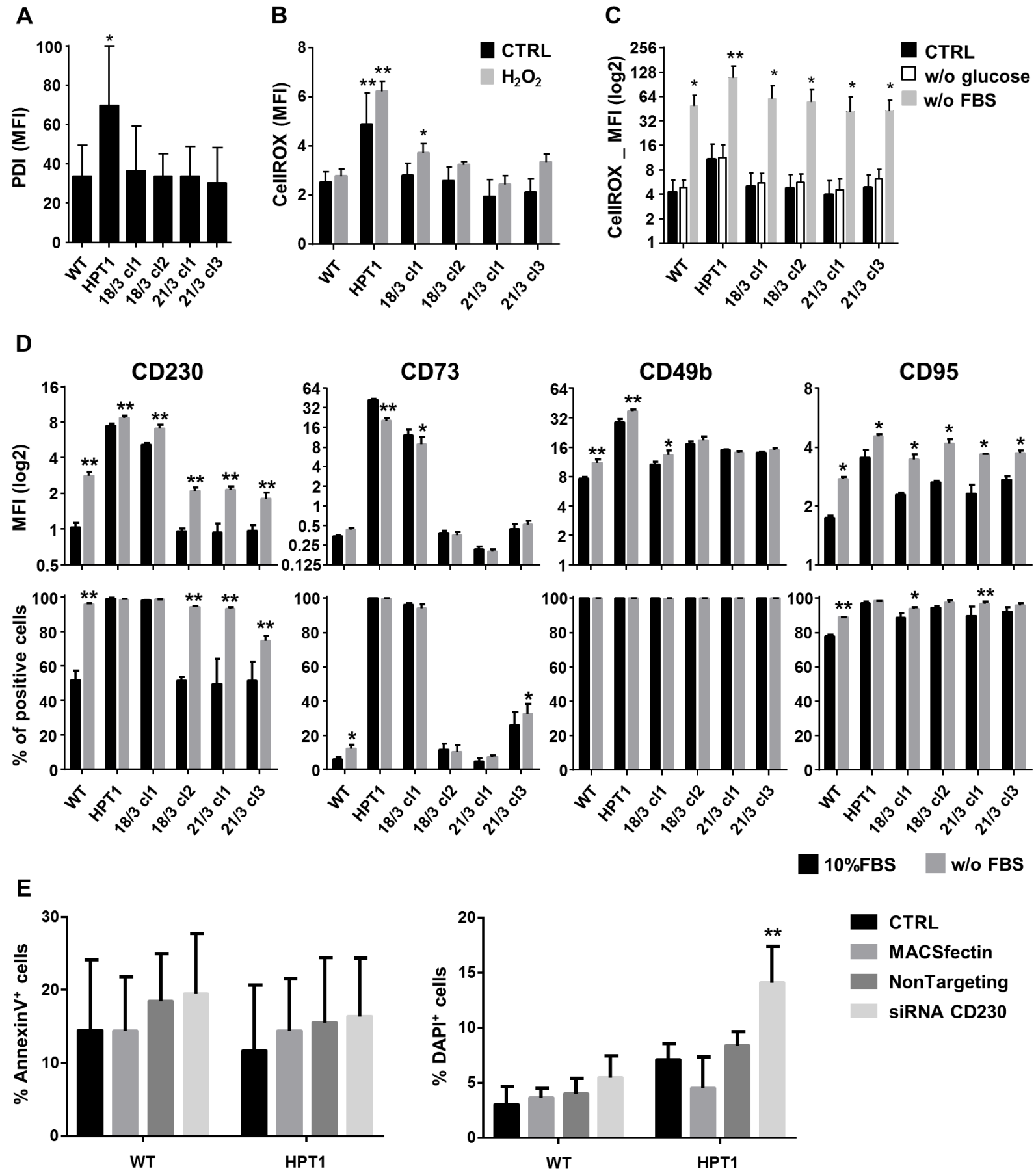


Figure 5



Cancer Research

The Journal of Cancer Research (1916–1930) | The American Journal of Cancer (1931–1940)

Cellular prion protein PRPC and ecto-5'-nucleotidase are markers of the cellular stress response to aneuploidy

Patrícia Henriques Domingues, Lalitha S Y Nanduri, Katarzyna Seget, et al.

Cancer Res Published OnlineFirst April 4, 2017.

Updated version	Access the most recent version of this article at: doi: 10.1158/0008-5472.CAN-16-3052
Supplementary Material	Access the most recent supplemental material at: http://cancerres.aacrjournals.org/content/suppl/2017/04/04/0008-5472.CAN-16-3052.DC1
Author Manuscript	Author manuscripts have been peer reviewed and accepted for publication but have not yet been edited.

E-mail alerts [Sign up to receive free email-alerts](#) related to this article or journal.

Reprints and Subscriptions To order reprints of this article or to subscribe to the journal, contact the AACR Publications Department at pubs@aacr.org.

Permissions To request permission to re-use all or part of this article, use this link <http://cancerres.aacrjournals.org/content/early/2017/04/04/0008-5472.CAN-16-3052>. Click on "Request Permissions" which will take you to the Copyright Clearance Center's (CCC) Rightslink site.